Phân tích nhiệt của cáp điện hạ áp có xét đến ảnh hưởng của sóng hài dòng điện

TÓM TẮT

Trong thiết kế và lựa chọn cáp điện hạ áp, ảnh hưởng của gia nhiệt do sóng hài dòng điện thường chưa được xem xét đầy đủ. Sự gia tăng của các phụ tải phi tuyến và nguồn năng lượng tái tạo làm tăng các thành phần dòng điện hài, dẫn đến điện trở xoay chiều và tổn hao Joule của cáp tăng lên, từ đó làm gia tăng nhiệt độ vận hành phụ thuộc vào biên độ và bậc hài. Khi có sóng hài, tổn hao trong ruột dẫn tăng, khiến nhiệt độ lõi cáp có thể vượt đáng kể so với trường hợp chỉ có dòng điện cơ bản. Trong nghiên cứu này, mô hình nhiệt ban đầu áp dụng cho cáp ngầm được cải tiến và hiệu chỉnh để phù hợp với đặc tính tản nhiệt của cáp PVC lắp đặt trên không, loại cáp phổ biến trong lưới điện hạ áp tại Việt Nam. Phổ dòng điện hài cùng các tham số nhiệt–điện của cáp được sử dụng làm dữ liệu đầu vào để đánh giá quá trình gia nhiệt dưới các điều kiện vận hành khác nhau. Nghiên cứu phân tích ảnh hưởng của sóng hài đến nhiệt độ lõi cáp, đánh giá sự suy giảm tuổi thọ cách điện và xem xét tác động của nhiệt độ môi trường. Trên cơ sở kết quả tính toán, mức giảm dòng điện vận hành phù hợp được đề xuất nhằm duy trì nhiệt độ cáp trong giới hạn cho phép, góp phần đảm bảo vận hành an toàn và hạn chế rủi ro suy giảm cách điện trong lưới điện hạ áp.

Từ khóa: *Cáp điện hạ áp, sóng hài dòng điện, đặc tính nhiệt, giới hạn vận hành, ước lượng tuổi thọ của cáp.*

Thermal Analysis of Low-Voltage Power Cables Considering the Presence of Current Harmonics

ABSTRACT

In practical design and selection of low-voltage power cables, the heating effects caused by current harmonics are often not sufficiently considered. In addition, with the increasing penetration of nonlinear loads and renewable energy sources in low-voltage distribution networks, harmonic current components tend to increase the AC resistance and Joule losses, thereby leading to a rise in cable operating temperature depending on the harmonic magnitude and order. When harmonics are present, the increased conductor losses may cause the actual cable core temperature to significantly exceed that observed under purely fundamental current conditions. In this study, a thermal model originally developed for underground cables is improved and its heat exchange parameters are recalibrated to accurately represent the thermal dissipation characteristics of overhead PVC-insulated low-voltage cables, which are widely used in Vietnamese distribution networks. By employing harmonic current spectra together with the electro-thermal parameters of the cable as input data, the proposed model enables the evaluation of cable heating behavior under various operating scenarios, while simultaneously considering variations in both harmonic magnitude and harmonic order. The study focuses on: (i) improving the thermal balance model for low-voltage cables; (ii) evaluating the impact of current harmonics on cable core temperature; (iii) analyzing insulation lifetime degradation under harmonic conditions; and (iv) assessing the influence of ambient temperature. Based on the numerical results, appropriate operating current derating levels are recommended to maintain cable temperature within permissible limits, thereby ensuring safe operating conditions and reducing the risk of insulation degradation in low-voltage power networks.

Keywords: *Low-voltage power cables, current harmonics, thermal characteristics, operating limits, cable lifetime estimation.*

1. INTRODUCTION

Low-voltage (LV) power cables are a critical component of distribution networks, forming the essential connection between substations and consumers in both residential and industrial sectors. Safe operation of these systems can be maintained only if conductor temperatures are kept within the allowable range. Prolonged thermal stress can, in turn, degrade operational safety and reduce the expected service life of the cables. When such conditions persist, insulation deteriorates more quickly, the lifetime of materials decreases, and faults including phase-to-phase short circuits or localized arc discharges may arise. These failures not only interrupt electricity supply but also cause considerable economic losses. For this reason, considerable research has been devoted to modeling cable thermal behavior with greater accuracy, focusing on aspects such as temperature distribution and heat dissipation, which are critical for the design, operation, and maintenance of power networks.[1-6]

In recent years, numerous studies have been directed towards enhancing the accuracy of thermal modeling for cables by considering real installation conditions that are more complicated than those assumed in standards. For instance, some research has examined the impact of air gaps in the cable structure,[7,8] or in real installations where conduits are not entirely filled,[9] showing that such aspects can notably augment the overall thermal resistance and lead to elevated operating temperatures compared to those predicted. In addition, some studies reevaluated the application of IEC standard formulas in unbalanced conditions[10] and in in cable trenches[11] with the aim of developing and suggesting more precise analytical models.

A further issue in modern grids concerns the impact of harmonics, which originate from the growing use of nonlinear loads and power electronic devices. Harmonics distort current waveforms, produce additional losses, and can raise conductor temperatures beyond the endurance of insulation. Research on cable thermal modeling has therefore examined harmonic effects on heating and proposed alternative installation practices or derating factors to mitigate them. For example,[12]

investigated the effect of harmonic currents produced by electric vehicle chargers on power systems. Other research calculated the temperature of low-voltage[13] and medium-voltage cables[14] by the thermal balance principle applied at every node of an equivalent thermal circuit. In the study by Ratheiser et *al.*,[15] the authors studied the effect of harmonic voltages on electric field distribution and temperature in medium voltage DC (MVDC) cable systems. In addition,[16] presented a dynamic thermal model for LV and MV cables under harmonic loads, revealing a noticeable decrease in ampacity and faster thermal response. Similarly, Alwan et *al.*[17] examined the thermal behavior of insulated cables in hot climates and found that harmonics could increase conductor temperature by up to 6°C and accelerate insulation aging, emphasizing the necessity of including harmonic-induced heating in ampacity assessments.

Most previous studies on the impact of harmonics have been limited to idealized current spectra or simplified load conditions, which do not accurately reflect real operating environments. To overcome this limitation, the present study investigates the thermal behavior of a low-voltage single-core Cadivi 0.6/1 kV cable arranged in a trefoil configuration and operating under free-air convection. Three groups of scenarios are considered. Case 1 analyzes the effect of individual harmonic orders while keeping the total RMS current constant, thereby assessing conductor temperature variation with harmonic order. Case 2 focuses on varying the total harmonic distortion (THD) of a fixed harmonic order to evaluate the influence of harmonic amplitude on temperature rise. Case 3 extends the analysis to a more practical scenario, in which the cable supplies current to a DC motor through a fully controlled bridge rectifier with variable firing angles, combining the effects of harmonics, load level, and ambient temperature. The combined results reveal that the conductor temperature depends not only on the RMS current magnitude or total harmonic distortion, but also on the harmonic order, spectral composition, and environmental conditions. These findings highlight the importance of incorporating harmonic spectral characteristics and nonlinear load conditions into thermal assessment and derating factor determination, as well as into accurate cable lifetime prediction, to ensure safe and reliable cable system operation.

The rest of this paper is structured as follows. Section 2 gives the thermal model used in this study. Section 3 outlines the cable parameters, installation conditions, and harmonic scenarios employed in the calculations. The results are analyzed in Section 4, and the conclusion is made in Section 5.

2. THERMAL MODELLING OF SINGLE-CORE CABLES

In this section, harmonic losses are first calculated using the frequency-dependent AC resistance. These results are then applied in a thermal circuit model to determine the conductor temperature of the single-core cable.

2.1. Harmonic loss calculation

The alternative current flowing through a conductor produces Joule losses. In the presence of harmonics, the total conductor loss in a cable can be determined as:

$$W_{total} = \sum_{h\geq 1} I_h^2 R_{AC}(h) \tag{1}$$

where I_h is the RMS current of the h- th harmonic and $R_{AC}(h)$ is the AC resistance for harmonic order h.

The AC resistance increases with frequency due to skin and proximity effects. According to IEC 60287-1-1, the AC resistance for a given harmonic order can be expressed as:

$$R_{AC}(h) = R_{DC}\left[1 + Y_s(h) + Y_p(h)\right] \tag{2}$$

where R_{DC} is the DC resistance of the conductor at the permissible maximum operating temperature per unit length (Ω/m), $Y_s(h)$ and $Y_p(h)$ are the skin effect and proximity effect factors, respectively.

$$Y_s(h) = \frac{x_s^4}{192 + 0.8x_s^4} \tag{3}$$

$$x_s^2(h) = \frac{8\pi f(h) k_s 10^{-7}}{R_{DC}} \tag{4}$$

$$Y_p(h) = \frac{x_p^4}{192 + 0.8x_p^4}\left(\frac{d_c}{S}\right)^2\left[0.312\left(\frac{d_c}{S}\right)^2 + \frac{1.18}{\frac{x_p^4}{192 + 0.8x_p^4} + 0.27}\right] \tag{5}$$

$$x_p^2(h) = \frac{8\pi f(h) k_p 10^{-7}}{R_{DC}} \tag{6}$$

where k_s is the coefficient factor for skin effect, k_p is the coefficient factor prolixity effect, d_c is the conductor diameter of the cable, S is the distance between core axes.

For low-voltage cables, dielectric losses are typically negligible, and since these cables do not include metallic sheaths or amours, associated losses do not occur. Consequently, harmonic loss calculations in LV cables focus solely on conductor losses arising from skin and proximity effects.

2.2. Cable thermal model

A generalized two-dimensional finite difference model (FDM) based on the principle of nodal heat balance in an equivalent thermal resistance network was developed in the study by Hiranandani.[18] The governing nodal heat balance equation can be expressed as:

$$\mathrm{W}_i + \sum_{j\in\{1,2,3;\, j\neq i\}}^{3}\left(\frac{\theta_j-\theta_i}{T_{ji}}\right)=0 \tag{7}$$

where W_i is defined as the summation of cable losses at node i, $\theta_j-\theta_i$ is the temperature difference between every two nodes and T_{ji} is the thermal resistance between every two nodes. The equivalent thermal circuit for a three-phase LV cable is illustrated in Figure 1.

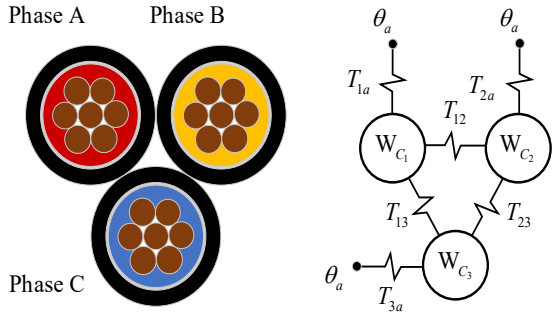

Figure1. The equivalent thermal circuit of cable.

According to Figure 1, there are three main heat flow paths for each conductor in the trefoil arrangement. As an example, the heat generated in phase A (W_{C_1}) is dissipated: (i) directly to the ambient through the external thermal resistance (T_{ia}), (ii) to phase B through the mutual thermal resistance (T_{12}), and (iii) to phase C through the mutual thermal resistance (T_{13}). The same principle applies to the other two conductors. By applying the nodal heat balance principle, the following equations can be written for each phase:

$$\theta_1-\theta_a = W_{C_1}T_{1a} \tag{8}$$

$$\theta_1-\theta_2 = W_{C_1}T_{12} \tag{9}$$

$$\theta_1-\theta_3 = W_{C_1}T_{13} \tag{10}$$

where $\theta_1,\theta_2,\theta_3$ are the conductor temperatures of phases A, B, and C, respectively, θ_a is the ambient temperature. T_{ia} is the total thermal resistance from conductor to ambient (including insulation, jacket, and convection), T_{1j} denotes the mutual thermal resistance between phase 1 and phase j. The thermal resistances can be calculated by IEC 60287-2-1.

The thermal resistance from the conductor core to the surface of its insulation:

$$T_i = \frac{\rho_i}{2\pi}\ln\left(1+\frac{2\delta}{d_c}\right) \tag{11}$$

The thermal resistance from the surface of the insulation to the outer jacket of the cable:

$$T_{ik} = \frac{\rho_i}{2\pi}\ln\left(\frac{d_o}{d_i}\right) \tag{12}$$

The mutual thermal resistance between conductors:

$$T_{\mathrm{ij}} = 2\left(T_i+T_{ik}\right) \tag{13}$$

In the studies by Gouda[13,14], the thermal resistance of the surrounding soil is employed to describe heat transfer from the cable surface to the external environment. In this study, the soil thermal resistance is replaced by a modified air thermal resistance, which more appropriately represents the heat dissipation mechanism of PVC-insulated cables installed in free air:

$$T_{air} = \frac{1}{\pi D_e^{*}\hbar\left(\Delta\theta_s\right)^{1/4}} \tag{14}$$

The total thermal resistance from conductor to ambient:

$$T_{ia} = T_i + T_{ik} + T_{\mathrm{air}} \tag{15}$$

where ρ_i the thermal resistivity of the insulation material (PVC), δ is the insulation thickness, d_c the conductor diameter, d_o is the jacket outer diameter, d_i is the jacket inner diameter, D_e^{*} is the jacket outer diameter in meter and $\hbar,\left(\Delta\theta_s\right)^{1/4}$ are the heat dissipation coefficient and the excess of cable surface temperature above ambient temperature which can be obtained in[20] respectively.

From Equations (8), (9), (10), and using the superposition principle, the following relation is obtained: $\frac{\theta_1}{T_{11}} - \frac{\theta_2}{T_{12}} - \frac{\theta_3}{T_{13}} = W_{C_1} + \frac{\theta_a}{T_{1a}}$

which $T_{11} = T_{22} = T_{33} = \frac{1}{T_{1a}} + \frac{1}{T_{12}} + \frac{1}{T_{13}}$ (16)

An analogous set of equations can be derived for phases B and C. Collectively, they form the thermal balance system can be represented in matrix form:

$$\begin{bmatrix} \frac{1}{T_{11}} & \frac{-1}{T_{12}} & \frac{-1}{T_{13}} \\ \frac{-1}{T_{21}} & \frac{1}{T_{22}} & \frac{-1}{T_{23}} \\ \frac{-1}{T_{31}} & \frac{-1}{T_{32}} & \frac{1}{T_{33}} \end{bmatrix} \begin{bmatrix} \theta_1(h) \\ \theta_2(h) \\ \theta_3(h) \end{bmatrix} = \begin{bmatrix} W_{C_1}(h) + \frac{\theta_a}{T_{1a}} \\ W_{C_2}(h) + \frac{\theta_a}{T_{2a}} \\ W_{C_3}(h) + \frac{\theta_a}{T_{3a}} \end{bmatrix} \quad (17)$$

where are the copper losses of each phase in the presence of harmonic order h. Hence, an increase in the cable core temperatures in the three phases due to h^{th} harmonics can be obtained:

$$\begin{bmatrix} \Delta\theta_1(h) \\ \Delta\theta_2(h) \\ \Delta\theta_3(h) \end{bmatrix} = \begin{bmatrix} \frac{1}{T_{11}} & \frac{-1}{T_{12}} & \frac{-1}{T_{13}} \\ \frac{-1}{T_{21}} & \frac{1}{T_{22}} & \frac{-1}{T_{23}} \\ \frac{-1}{T_{31}} & \frac{-1}{T_{32}} & \frac{1}{T_{33}} \end{bmatrix}^{-1} \begin{bmatrix} W_{C_1}(h) + \frac{\theta_a}{T_{1a}} \\ W_{C_2}(h) + \frac{\theta_a}{T_{2a}} \\ W_{C_3}(h) + \frac{\theta_a}{T_{3a}} \end{bmatrix} - \theta_a \begin{bmatrix} 1 \\ 1 \\ 1 \end{bmatrix} \quad (18)$$

Then, the cable core temperatures of the three phases with harmonics can be obtained:

$$\begin{bmatrix} \theta_{t1} \\ \theta_{t2} \\ \theta_{t3} \end{bmatrix} = \theta_a \begin{bmatrix} 1 \\ 1 \\ 1 \end{bmatrix} + \begin{bmatrix} \sum_{h=1}^{\infty} \Delta\theta_1(h) \\ \sum_{h=1}^{\infty} \Delta\theta_2(h) \\ \sum_{h=1}^{\infty} \Delta\theta_3(h) \end{bmatrix} \quad (19)$$

The developed thermal model is subsequently applied to investigate the impact of harmonic currents on the thermal behavior of the cable.

3. SIMULATION SETUP AND HARMONIC SCENARIOS

Section 3 presents the simulation setup used in the investigation of the thermal response of the single-core cable subjected to harmonic excitations. The first section refers to the adopted cable and cable characteristics, including its electric, thermal, and installing attributes. The second section refers to the harmonic conditions considered.

3.1. Cable parameters

The analysis is carried out on a low-voltage single-core Cadivi cable rated at 0.6/1.0 kV, installed in free air and arranged in a trefoil configuration. Both the insulation and outer sheath are made of PVC, and according to IEC 60502-1, the maximum continuous operating temperature for this material is 70°C. The ambient temperature is assumed to be θ_a = 30°C. The cable has a nominal cross-sectional area of 70 mm^2 and a rated current of I_{rated} = 219 A. The principal geometrical dimensions and thermal–electrical properties employed in the simulations are summarized in Table 1.

Table 1. Parameters of the cable.

Parameter	Value	Units
ρ_i	6.5	K × m/W
δ	1.4	mm
d_c	9.7	mm
d_i	12.5	mm
d_o	15.3	mm
S	15.3	mm
R_{DC}	0.268	mΩ/m

3.2. Harmonic case studies

To investigate the thermal impact of harmonics on the single-core cable, two groups of case studies are designed with complementary purposes.

3.2.1. Case 1 – effect of individual harmonic orders

In this group, the conductor temperature is evaluated under two conditions: (i) only the fundamental component at 50 Hz is present (without harmonics) and (ii) the fundamental component is superimposed with harmonic components of orders $6n \pm 1$ (e.g., 5^{th}, 7^{th}, 11^{th}, 13^{th}, etc.), which typically occur in three-phase systems. The total RMS current per phase is kept equal to the rated current, I_{rated} = 219 A. To examine the effect of harmonic order, THD is held constant while the harmonic order h is varied. Thus, Case 1 reveals how conductor heating changes with harmonic order for a given harmonic amplitude.

3.2.2. Case 2 – single-harmonic thd variation

In this group, the conductor temperature is evaluated when the fundamental component at 50 Hz is superimposed with only one harmonic order from the sequence $6n \pm 1$. The total RMS current per phase is maintained equal to the

rated current, I_{rated} = 219 A. To assess the effect of harmonic amplitude, the harmonic current (expressed as THD) is varied across multiple levels while keeping the harmonic order fixed.

3.2.3. Case 3 – controlled rectifier-motor system simulation

In this case, the cable temperature is studied under practical operating conditions through a simulated system that includes a three-phase low-voltage supply, a fully controlled bridge rectifier, and a DC motor. By adjusting the firing angle of the rectifier, the current waveform on the AC side becomes increasingly distorted, which reflects different motor loading conditions. These current waveforms, containing both the fundamental and harmonic components, are then applied to the thermal model to estimate the conductor temperature. This case serves to connect the previous harmonic-based analyses with a more realistic industrial scenario.

Two operating scenarios are examined. In the first, the cable temperature is evaluated with and without harmonics at load levels ranging from 0% to 100% of the rated current to determine a suitable derating factor. In the second, the ambient temperature is varied from 20°C to 40°C, representing tropical climatic conditions in Da Nang, Vietnam, to assess the effect of environmental temperature on cable thermal limits.

For each condition, the conductor temperature and cable lifetime are estimated, allowing comparison between operation with and without harmonics. These results help to clarify how both harmonic distortion and ambient temperature jointly influence cable loading capability in practical applications.

For Case 1 and Case 2, the thermal calculations are carried out directly in MATLAB by parametrically defining the current harmonic components (magnitudes and orders) and applying them to the thermal model described by Eq. (19). For Case 3, the current waveforms are obtained from a MATLAB/Simulink model of a controlled rectifier–motor system, and the corresponding harmonic spectra are extracted using Fast Fourier Transform analysis before being used as inputs to the same thermal model.

4. RESULTS AND DISCUSSION

This section presents the simulation results obtained from the thermal model introduced in Section 2 under the harmonic scenarios defined in Section 3.

4.1. Combined effect of harmonic order and current amplitude on conductor temperature

The values for Case 1 and Case 2 are depicted in Figures 2 and 3, respectively. The plots in the graphics collectively reveal the effects of the harmonic order h and the harmonic current amplitude I_h on the temperature of the conductors, while the overall RMS current per phase remains the same at 219 A.

In Figure 2, the curves show how the conductor temperature changes with harmonic

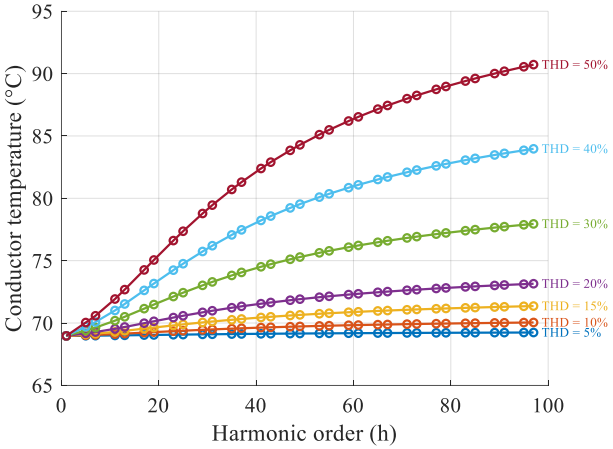

Figure 2. Variation of conductor temperature with harmonic order for different THD levels.

orders of the form $6n \pm 1$ (such as the 5^{th}, 7^{th}, 11^{th}, 13^{th}, and so on) for different THD levels. Since the harmonic current follows $I_h = THD \times I_1$, a higher THD means a larger harmonic current amplitude and a smaller fundamental current I_1, while the total RMS current remains unchanged. It can be noted that for the same harmonic order, larger harmonic currents generate more heat inside the conductor, which results in a higher temperature rise. Such a relationship follows Joule's law, in which the power dissipation is proportional to the square of the current magnitude.

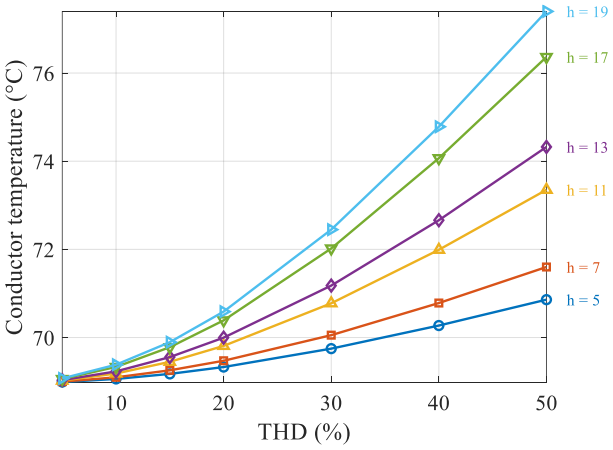

Figure 3. Variation of conductor temperature with THD for different harmonic orders.

Figure 3 illustrates the complementary relationship: each curve is related to a given harmonic order, while the THD varies to mimic changing harmonic amplitudes. On inspecting curves for the same THD levels (i.e., corresponding current amplitudes), it is clear that the temperature increases with harmonic order, so higher-order harmonics have a greater contribution to heating. This result occurs because the AC resistance $R_{AC}(h)$ significantly increases when the frequency increases, by virtue of the skin and proximity effects that become greater for higher harmonic orders and so result in an increase in Joule losses.

Considering the two plots together offers clearer insight into how harmonics influence the cable's heating behavior. The results show that as both the harmonic order and current amplitude rise, each harmonic adds extra loss to the conductor, which raises its temperature. Hence, ignoring higher-order harmonics in real operation can lead to underestimating the actual temperature of the cable.

4.2. Thermal behavior in controlled rectifier–motor drive system (Case 3)

According to the results of Case 3 shown in Figure 4, changes in the rectifier's firing angle leads to variations in the DC motor load, and this change directly influences the harmonic distortion (THD) of the AC-side current. When the firing angle becomes larger, the current waveform departs further from the sinusoidal shape, its THD rises, while the overall current amplitude drops. Because of this reduction in current, the heat generated in the conductor also decreases, and the cable temperature gradually falls as the firing angle increases.

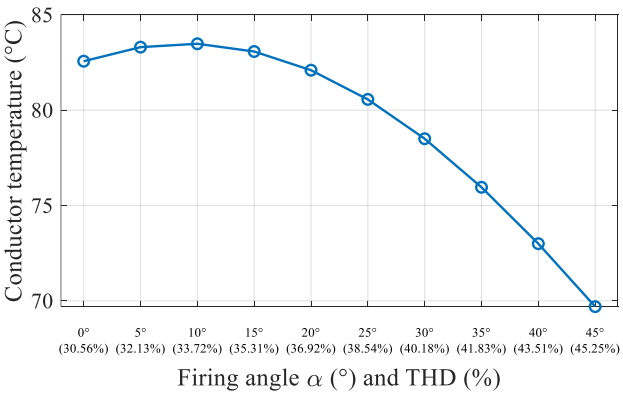

Figure 4. Variation of conductor temperature with firing angle.

Even so, the temperature values remain above the allowable operating limit of 70°C throughout the entire range of operation. This indicates that the presence of harmonic components increases the total electrical losses enough to push the cable into a state of thermal overload, even though the current itself is reduced. To maintain safe operation, both the load level and the harmonic content need to be considered, and suitable control or filtering measures should be applied to keep the cable temperature within acceptable limits.

4.3. Effect of load level with and without harmonics

Figure 5 clearly shows that the presence of harmonic distortion causes the conductor to operate at a consistently higher temperature compared with the case of a pure sinusoidal current. This occurs even though both cases are evaluated using the same total RMS current. The rise in temperature can be attributed to additional losses generated by higher-frequency current components, which increase the effective AC resistance of the conductor.

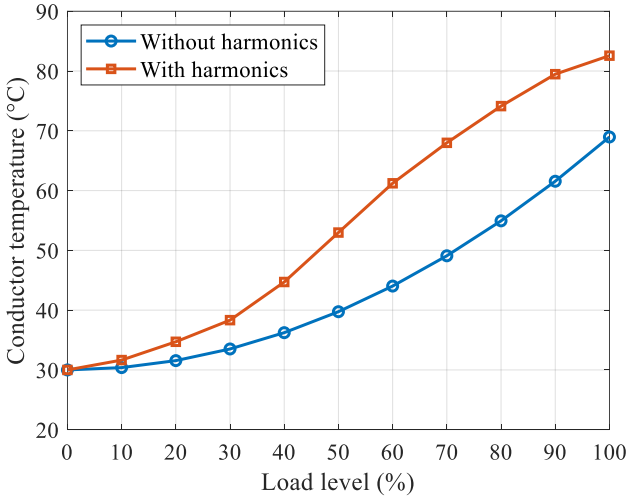

Figure 5. Conductor temperature variation with load level under harmonic and non-harmonic conditions.

To maintain the conductor temperature within the permissible limit, the operating load should be reduced to approximately 70–80% of the rated value. Another option is to select a cable type with a higher ampacity. These observations emphasize that harmonic effects must be accounted for during both cable selection and system operation, especially in networks feeding nonlinear loads such as converters or inverters.

To assess how this temperature increases influences insulation aging, the Arrhenius law is applied to estimate the decline in cable lifetime

as the operating temperature rises under overload. The relationship is formulated as:

$$L(T_{op}) = L_{ref} exp\left(\frac{E_a}{k_B}\left(\frac{1}{T_{op}} - \frac{1}{T_{ref}}\right)\right) \quad (20)$$

where $L_{ref} = 20$ years at $T_{ref} = 70°C = 343K$, $E_a = 0.7eV$ is the activation energy of the PVC material, and $k_B = 8.617\times10^{-5} eV/K$ is the Boltzmann constant. The estimated lifetimes obtained from the simulated temperatures are summarized in Table 2, comparing harmonic and non-harmonic cases at different load levels.

Table 2. Cable lifetime estimation for various load levels.

Load level	Without harmonics (years)	With harmonics (years)
70%	93.72	22.98
80%	59.07	15.22
90%	35.2	10.91
100%	21.48	8.65

The data reveals a clear degradation trend: the presence of harmonics shortens the insulation lifetime considerably. For an identical loading condition, the expected lifetime under harmonic operation drops to roughly 40–50% of that in a purely sinusoidal case. At rated load, the cable lifetime decreases from 20 years to about 8 years, indicating strong thermal aging induced by harmonic-related overheating. Consequently, in practical operation involving loads with nonlinear components, it is necessary to determine an appropriate derating level to ensure the long-term reliability of the cable and the electrical system.

4.4. Influence of ambient temperature

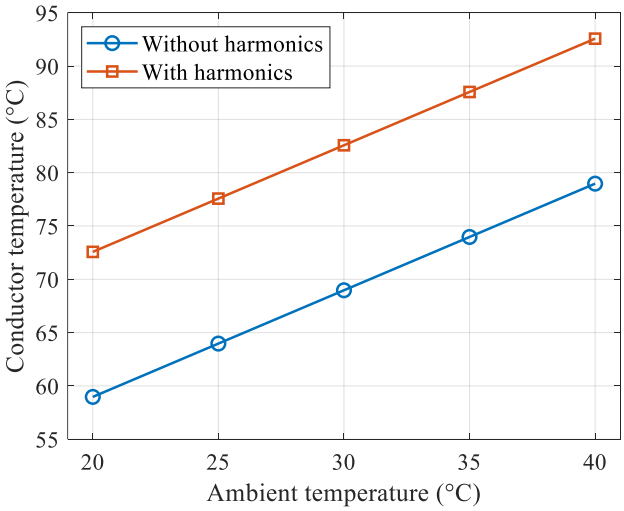

Figure 6. Effect of ambient temperature on conductor temperature.

Figure 6 shows how the cable core temperature varies with ambient temperature once thermal equilibrium is reached. Since the cable is placed in a real thermal environment, its core temperature naturally depends on the surrounding conditions. For that reason, ambient temperature should be treated as an operating variable rather than a fixed constant. In practice, ambient temperature fluctuates from time to time, but the cable core does not follow those short-term changes immediately because of its thermal inertia. When the surrounding temperature stays roughly constant for a period much longer than the cable's thermal time constantly-say, over a day or a season, the core temperature gradually settles to a steady value. Therefore, using steady-state core temperatures associated with average ambient conditions is a reasonable way to describe the long-term thermal behavior of the cable.

At steady operation, when the core temperature remains nearly constant, the insulation material ages faster as the temperature increases, following the Arrhenius law. Based on that relation, the expected service life of the cable, both with and without harmonic components, was evaluated at several ambient temperature levels. The calculated results are summarized in Table 3.

From Table 3, it can be observed that higher ambient temperatures correspond to a shorter cable lifetime, reflecting how insulation materials naturally deteriorate under heat. The influence of harmonics varies with temperature: at lower ambient levels, their impact is minor, but as the environment becomes hotter, harmonic losses intensify, leading to a faster reduction in service life. Therefore, in practical operation, in addition to the derating effect caused by harmonics, the cable load should also be adjusted according to ambient temperature conditions to ensure its durability and service lifetime.

Table 3. Conductor lifetime under different ambient conditions.

Ambient temperature (°C)	Without harmonics (years)	With harmonics (years)
20	43.35	16.12
25	30.16	12.33
30	21.21	8.90
35	15.07	6.47
40	10.81	4.47

4.5. Comparative discussion

The three case studies reveal that the thermal response of single-core cables to harmonic distortion depends on multiple interacting

factors, including the harmonic order, current level, load, and ambient temperature. As seen in Sections 4.1 and 4.2, higher-order harmonics intensify the skin and proximity effects, thereby increasing the effective AC resistance and raising the conductor temperature even when the RMS current remains unchanged. Extending these observations to the rectifier–motor system in Case 3 leads to the same pattern: when the current waveform becomes more distorted (i.e., higher THD), the conductor operates at a higher temperature despite a smaller overall current.

The comparison between Sections 4.3 and 4.4 shows that both load and ambient temperature amplify the influence of harmonics. At heavier loads, the added harmonic losses drive the operating temperature above safe limits, cutting the expected insulation lifetime to roughly half of that under pure sinusoidal conditions. As the ambient temperature rises, insulation aging accelerates, and the additional heating due to harmonics becomes more evident–an effect that deserves attention in warm or tropical environments where cables often run close to their thermal capacity.

Taken together, these results underline that harmonic effects have a lasting influence on cable thermal performance. Evaluating cable ratings solely from the RMS current can underestimate the true conductor temperature and the rate of insulation aging. In practical operation, both harmonic distortion and ambient temperature must be considered in load limit settings to ensure safe performance and long-term reliability of the cable system.

5. CONCLUSION

This study evaluated the thermal behavior of low-voltage single-core cables under harmonic current loading using an improved steady-state thermal model adapted for overhead PVC-insulated cables. The analysis showed that harmonic currents significantly increase the AC resistance through enhanced skin and proximity effects, thereby producing additional thermal losses even when the RMS current remains unchanged. As a result, the conductor temperature may exceed its allowable limit under nonlinear loading conditions, accelerating insulation ageing and reducing cable lifetime. This adverse effect becomes more pronounced at elevated ambient temperatures, which is typical in tropical operating environments. The findings indicate that current ratings based solely on RMS values do not adequately represent the actual thermal stress experienced by cables in the presence of harmonics. Accordingly, appropriate current-derating measures should be considered based on both the harmonic spectrum and the ambient temperature to ensure thermal safety and long-term operational reliability.

Future studies will focus on adding dynamic and transient aspects to the model so that temperature variations over time can be represented more accurately. In addition, finite element (FEM) techniques will be applied to examine detailed temperature fields within the cable. A combination of numerical modeling and experimental validation is expected to offer a more detailed understanding of the electro–thermal interaction under harmonic-rich conditions.

REFERENCES

1. J. Wang, Y. Liang, C. Ma. A novel transient thermal circuit model of buried power cables for emergency and dynamic load, *Energy Reports*, **2023**, *9*, 963–971.
2. G. Petrović, M. Cvetković, T. Garma, T. Kilić. An approach to thermal modelling of power cables installed inducts, *Electric Power Systems Research*, **2023**, *214*, 108916.
3. W. Wang, X. Bai, W. Si, Y. Zhao, W. Yao, G. Liu, H. Liu, L. Yan, D. Yang, X. Meng, Y. Xu, C. Fu. *Review of calculation methods of power cables temperature based on thermal circuit model*, 2024 IEEE 7th Advanced Information Technology, Electronic and Automation Control Conference (IAEAC 2024), Chongqing, China, 2024.
4. Y. B. Demirol, O. Kalenderli. Investigation of effect of laying and bonding parameters of high-voltage underground cables on thermal and electrical performances by multiphysics FEM analysis, *Electric Power Systems Research*, **2024**, *227*, 109987.
5. Y. S. Kim, H. N. Cong, B. H. Dinh, H. K. Kim. Effect of ambient air and ground temperatures on heat transfer in underground power cable system buried in newly developed cable bedding material, *Geothermics*, **2025**, *125*, 103151.
6. E. Mustafa, U. Ibrahim, N. Ahmed, I. Ahmed, A. R. Abbasi, A. Nawaz, M. F. Abbas, Z. Á. Tamus. Thermal degradation and multi-performance aging assessment of low voltage nuclear cable, *Electric Power Systems Research*, **2026**, *250*, 112128.
7. P. Wang. Optimization for thermal rating method of high voltage cable considering the existence of air gap, *Electric Power Systems Research*, **2023**, *217*, 109151.
8. M. V. S. da Silva, O. M. O. de Araújo, C. M. S. F. F. dos Santos, D. F. de Oliveira, C. M. Freitas, R. T. Lopes. Evaluation of low voltage on electrical cables using microct and COMSOL Multiphysics, *Radiation Physics and Chemistry*, **2024**, *224*, 112067.

9. M. Quercio, J. C. D. P. Lopez, S. Grasso, A. Canova. Numerical and experimental analysis of thermal behaviour of high voltage power cable in unfilled ducts, *Scientific Reports*, **2024**, *14*, 20599.
10. R. Hu, G. Liu, Z. Xu, P. Wang, H. Zeng, W. Ye. Improved thermal analysis for three-core cable under unbalanced three-phase loads, *Electric Power Systems Research*, **2023**, *216*, 108964.
11. S. Xu, S. Tao, Y. Xu. Secondary sideband harmonic emission characteristics of individual/multi-parallel grid-connected inverters, *International Journal of Electrical Power and Energy Systems*, **2025**, *170*.
12. H. Wang, W. Zhou, K. Qian, S. Meng. Modelling of ampacity and temperature of MV cables in presence of harmonic currents due to EVs charging in electrical distribution networks, *International Journal of Electrical Power & Energy Systems*, **2019**, *112*, 127–136.
13. O. E. Gouda, A. Z. E. Dein. Enhancement of the thermal analysis of harmonics impacts on low voltage underground power cables capacity, *Electric Power Systems Research*, **2022**, *204*, 107719.
14. O. E. Gouda, A. Z. E. Dein, E. Tag-Eldin, M. Lehtonen, M. M. F. Darwish. Thermal analysis of the influence of harmonics on the current capacity of medium-voltage underground power cables, *Energy Science & Engineering*, **2023**, *11*(10), 3471–3485.
15. P. Ratheiser, S. Shahtaj, U. Schichler, B. G. Stewart. *Harmonics in MVDC cable systems – study on thermal and electric stress*, The 23rd International Symposium on High Voltage Engineering (ISH 2023), Glasgow, United Kingdom, 2023.
16. G. F. A. Osman, T. M. Z. Elsharkawy, W. A. A. Salem. *Thermal analysis of underground distribution cables under dynamic loading in the presence of harmonic load currents*, The 22nd International Middle East Power Systems Conference (MEPCON), Assiut, Egypt, 2021.
17. S. H. Alwan, A. K. Jasim, Y. F. Hassan. Thermal behavior of insulated cables under the influence of harmonics in hot countries, *International Journal on Energy Conversion*, **2024**, *12*(1), 24–31.
18. A. Hiranandani. Calculation of conductor temperatures and ampacities of cable systems using a generalized finite difference model, *IEEE Transactions on Power Delivery*, **1991**, *6*(1), 15–24.